UDK 620.1:67.017:669.018.4
Original scientific article/Izvirni znanstveni članek

ISSN 1580-2949
MTAEC9, 55(2)305(2021)

MICROSTRUCTURE AND MECHANICAL PROPERTIES OF REFRACTORY HIGH-ENTROPY ALLOY HfMoNbTiCr

MIKROSTRUKTURA IN MEHANSKE LASTNOSTI VISOKO-ENTROPIJSKE OGNJEVZDRŽNE ZLITINE HfMoNbTiCr

Jiaojiao Yi[1], Lu Wang[2], Mingqin Xu[1], Lin Yang[2*]

[1]School of Mechanical Engineering, Jiangsu University of Technology, 1801 Zhongwu Road, Zhonglou District, Changzhou 213001, P. R. China
[2]School of Materials Science and Engineering, Jiangsu University of Technology, 1801 Zhongwu Road, Zhonglou District, Hangzhou 213001, P. R. China

Prejem rokopisa – received: 2020-10-06; sprejem za objavo – accepted for publication: 2020-12-29

doi:10.17222/mit.2020.197

A new refractory alloy, HfMoNbTiCr, was obtained by replacing Zr with Cr or Mo in the HfMoNbTiZr or HfNbTiCrZr alloys using vacuum arc melting. The phase components, microstructures and compressive properties of the alloy in the as-cast and annealed states were investigated. The results showed that the phase components changed from a single BCC phase in HfMoNbTiZr and BCC+Laves phases in HfNbTiCrZr to multiple phases – primarily two BCC phases and two cubic Laves phases – in HfMoNbTiCr. Notably, the yield and ultimate compressive strength of the as-cast alloy significantly increased from 1719 and 1803 MPa to 1851 and 2489 MPa, without a decrease in the ductility. The stress fields induced by Mo and the Cr-containing Laves phases were responsible for the enhanced strength, while the stiff network-like framework composed of intrinsically-strong Cr-containing Laves phases may have played a vital role in retaining the ductility.

Keywords: refractory high-entropy alloys, phase components, microstructure, mechanical properties

Avtorji v članku poročajo o izdelavi novih ognjevzdržnih zlitin tipa HfMoNbTiCr, v katerih so zamenjali Zr s Cr ali Mo v HfMoNbTiZr ali HfNbTiCrZr zlitinah. Zlitine so izdelovali s postopkom obločnega pretaljevanja. Raziskali so fazno sestavo, mikrostrukturo in mehanske lastnosti zlitin v litem in žarjenem stanju. Rezultati raziskav so pokazali, da se fazna sestava zlitine HfMoNbTiZr spremeni iz enovite BCC faze in BCC+Lavesove faze v HfNbTiCrZr, ter zlitini HfMoNbTiCr v večfazni primarno dvo-fazni BCC sistem in v dve kubični Laves fazi. Ugotavljajo, da sta se tlačna meja plastičnosti in tlačna trdnost pri porušitvi zlitine v litem stanju znatno zvišali iz 1719 MPa oziroma iz1803 MPa na 1851 MPa oziroma na 2489 MPa, brez da bi se pri tem zmanjšala duktilnost zlitin. Napetostna polja, inducirana z Lavesovimi fazami, ki vsebujejo Mo in Cr, ki sta odgovorna za povišanje tlačne trdnosti obeh zlitin medtem, ko togo, mreži podobno ogrodje, sestavljeno iz notranje močnih Lavesovih faz, ki vsebujejo Cr, igrajo odločilno vlogo pri ohranitvi duktilnosti.

Ključne besede: visoko-entropijske ognjevzdržne zlitine, fazna sestava, mikrostruktura, mehanske lastnosti

1 INTRODUCTION

Inspired by innovative metallurgical processes, high-entropy alloys (HEAs) emerged in the past decade as a group of alloys with superior properties,[1–4] i.e., good room-temperature ductility,[5,6] high strength at elevated temperatures[7,8] and improved oxidation resistance.[9] HEAs are commonly defined as alloys with ≥5 major elements ranging from 5–35 *x*/%.[10,11] Due to high demands for the materials at elevated temperatures in the aerospace and petrochemical industries, refractory HEAs, represented by NbMoTaW and VNbMoTaW, were first proposed by D. B. Miracle and O. N. Senkov et al.[12,13] They possess simple body-centered cubic (BCC) structures, outstanding yield strengths of 405 MPa and 477 MPa at 1600 °C and densities greater than 9.0 g/cm^3. Later, the HfNbTaTiZr alloy, also with a BCC phase structure, exhibited an excellent ductility exceeding 50 % but a lower strength than the first two refractory HEAs.[14]

Optimizing the alloy composition with an elemental addition or substitution for a given base alloy is an effective way to enhance material properties;[15,16] thus, adjusting the alloy composition became a method for perfecting the mechanical properties of HEAs.[17,18] O. N. Senkov et al.[8] used Al to replace Hf in the HfNbTaTiZr alloy, which significantly increased the yield strength and hardness (98 % and 29 %), accompanied by a lower density (9 %).[8] In addition, the important role of Al in tuning the mechanical properties of HfNbTaTiZr alloys was also confirmed with an equiatomic HfNbTaTiZrAl alloy,[19] which exhibited a high yield strength of 1500 MPa under compression carried out by C. M. Lin et al.[19] In fact, the substitution by or addition of other elements, such as Mo, Cr, Zr, and V, also play vital roles in regulating and controlling the properties of different multi-component base alloys. For example, É. Fazakas et al.[6] found that the substitution of Ta by Cr enhanced the strength and hardness of a refractory HEA, HfNbTiCrZr, due to the formation of Cr-containing Laves phases (Cr_2Hf, Cr_2Nb) during casting. Additionally, N. N. Guo et al.[20] recently reported a new refractory HEA, HfMoNbTiZr, obtained

*Corresponding author's e-mail:
yanglin@jsut.edu.cn (Lin Yang)

by completely replacing Ta with Mo in HfNbTaTiZr.[20] This new alloy exhibited a single BCC phase structure and showed a greatly enhanced yield strength of 1575 MPa, increased ductility and a fracture strain of 9.08 %.[20]

The previously-reported alloys, HfMoNbTiZr or HfZrNbTiCr, showed excellent yield strengths. To further enhance their mechanical properties, in this work, a new refractory HEA, HfMoNbTiCr, was made using Cr or Mo to completely substitute Zr. The replacement of Zr with Cr (Laves-phase formation) or Mo (high Young's modulus) in the base alloy considerably increased the yield and fracture strengths of the resulting alloy.

2 EXPERIMENTAL PART

HfMoNbTiCr alloy ingots were prepared with vacuum-arc-melted equimolar mixtures of the the corresponding elements. Hf, Mo, Nb, Ti, and Cr were bulk slugs with purities of (99.99, 99.9 , 99.95, 99.95, and 99.9) % (*w*/%), respectively. Cylindrical samples were sucked into a water-cooled copper crucible with dimensions of Φ4×60 mm under a titanium getter argon atmosphere. The detailed preparation process can be found in our previous study.[4] Energy-dispersive spectrometry (EDS) showed that the actual composition of the cylindrical specimens was $Hf_{19.7}Mo_{23.2}Nb_{18.0}Ti_{20.7}Cr_{18.4}$, which was similar to the nominal composition. Annealing was conducted at 1273 K for 20 h under vacuum to homogenize the microstructure of the as-cast samples.

The phase components of the as-cast and annealed samples were identified with a Rigaku X-ray diffractometer with a 2θ range of 20–100° and a scanning rate of 3°/min. The microstructure was analysed with a Zeiss Sigma 500 scanning electron microscope (SEM). Vickers-microhardness values were measured using an HVS-1000B tester under a load of 50 g for 10 s. The room-temperature compressive properties were evaluated using a computer-controlled testing machine (Instron, Norwood, MA) with a constant ramp speed of 5.6×10^{-3} mm/s and an initial strain rate of 10^{-3} s^{-1}. The tested compressed samples had dimensions of (Φ3.7×5.6) mm.

3 RESULTS

3 Results and discussion

3.1 Phase analysis

Figure 1 shows the XRD patterns of the studied as-cast and annealed HfMoNbTiCr alloys (a–b), and the previously reported HfZrNbTiCr and HfMoNbTiZr (c–d) alloys.[6,20] In addition to the HfTaNbTiZr alloy,[19] the HfMoNbTiZr alloy, in which Mo was used to substitute Ta, also exhibited a simple BCC microstructure (**Figure 1d**), but its strength increased from 929 MPa to 1575 MPa.[14] The pattern of HfNbTiZrCr shows that when Ta was substituted by Cr, several new diffraction peaks appeared, corresponding to Cr-rich Laves phases

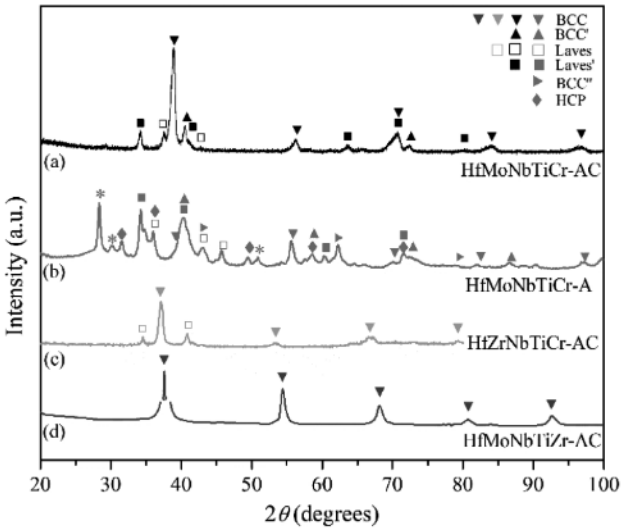

Figure 1: XRD patterns of the currently studied as-cast (AC) and annealed (A) HfMoNbTiCr alloys (a–b), together with the reported HfZrNbTiCr and HfMoNbTiZr (c–d) alloys[6,20]

(the C15 type: Cr_2Nb and Cr_2Hf) and accompanied by BCC peaks in accordance with the JCPDS cards (**Figure 1c**).[6] The emerged Laves phases were closely related to the atomic-size ratio and the atomic ratio in an alloy larger than 1.225 is beneficial to the formation of a Laves phase.[21] For HfNbTiZrCr, the atomic ratio of Hf and Cr (1.271) was attributed to the formation of the Cr-rich Laves phases, which were shown to greatly enhance the strength of some refractory HEAs.[22] Since both Mo and Cr-rich Laves phases enhance the mechanical properties, HfMoNbTiCr was designed by replacing Zr in HfCrNbTiZr and HfMoNbTiZr with Mo or Cr. According to the XRD pattern, the phase components of the as-cast HfMoNbTiCr were identified as two BCC and two cubic Laves phases (**Figure 1a**). According to the JCPDS cards, one Laves phase matched with the C15-type Cr_2(Hf, Nb) cubic Laves phase, with a lattice parameter of a = 700.6 pm, while the other Laves phase corresponded to Mo_2Hf, with a lattice parameter of a = 740.9 pm. The BCC and BCC' phases matched well with MoNb/NbTi and MoTi/TiCr, with lattice parameters of a = 327.3 pm and a = 314.4 pm, respectively. The BCC phases were still the majority phase (73.5 %) in the HfMoNbTiCr alloy, according to the Equation:

$$W_{pi} = (p / \Sigma p_i) \times 100\ \% \quad (1)$$

Where W_{pi} is the volume fraction of the ith phase, p is the peak intensity of a given phase in the XRD pattern, i is the number of the phase, and Σp_i is the total peak intensity of all the phases in the XRD pattern. Thus, we conclude that the incorporation of Mo boosted the formation of BCC phases.

After annealing, the number of diffraction peaks significantly increased compared with the XRD pattern of the original as-cast alloy, especially at $2\theta < 65°$ (**Figure 1b**). Without considering the few unknown peaks,

the phase components were unambiguously identified as belonging to six phases, including three BCC phases (BCC, BCC', and BCC''), two cubic Laves phases (Laves and Laves') and one hexagonal close-packed (HCP) phase. According to the JCPDS cards, the BCC phase corresponded to a Nb-rich BCC phase with a lattice parameter a = 331.2 pm. The BCC' phase was in agreement with the MoTi/TiCr BCC' in the as-cast state, as evidenced by the almost identical lattice parameter a = 317.4 pm. The BCC'' phase was rich in Cr and Mo and had a relatively small lattice parameter a = 297.0 pm due to the small atomic radius of Cr.

Likewise, the two Laves phases were identified as Cr_2(Hf, Nb) and Mo_2Hf cubic Laves phases, which were also identical to those in the as-cast alloy. The HCP phase matched with Hf HCP with lattice parameters a = 315.0 pm/c = 498.4 pm, which might have stemmed from the breaking of the solution limit of Hf in the BCC phases. Thus, compared with the phase components of the as-cast alloy, the presence of the new BCC and HCP phases in the annealed alloy implied that the microstructure of the initial as-cast alloy was far from equilibrium. This shows that post-process annealing was necessary to establish the number and types of phases at equilibrium.[1] However, there are currently no standard thermal treatments to ensure that equilibrium is reached, and this must be comprehensively investigated.

3.2 Microstructure

The microstructures of the as-cast and annealed alloys are shown in **Figure 2**, respectively. A typical dendrite structure with an average primary arm size of around 5 μm was observed in the as-cast HfMoNbTiCr (**Figures 2a** to **2b**). Apparently, the dendritic regions (grey regions marked as D) were irregularly embedded into a relatively continuous interdendritic region (bright part marked as ID). The volume fraction of the dendritic regions was much higher than that of the interdendritic regions. After annealing, the microstructures were still composed of dendrites (grey regions marked as D as shown in **Figures 2c** to **2d**) and discontinuous interdendrites (bright region marked as ID). However, many more slim-strip interdendrites were present along the bulky interdendrites (marked with red arrows) than in the original as-cast alloy.

In order to determine the elemental distribution in the alloy, EDS maps of the as-cast and annealed alloys were obtained and are shown in **Figure 3**. For the as-cast alloy, the maps show that the dendritic regions are mainly rich in Nb and Mo with the top second highest melting point among all the principal elements. The interdendritic regions are enriched with Hf and Cr with a relatively low melting point. Moreover, most of Ti was distributed in the dendrites, but some was segregated at the boundaries between the dendrites and interdendrites to form 1–2 μm thick transition layers (marked with arrows in the Ti map in **Figure 3f**). Similar Ti-rich transition layers were observed with BCC crystal structures in a hot isostatically pressed $NbCrMo_{0.5}Ta_{0.5}TiZr$ alloy.[22] For the annealed alloy, the dendritic regions were mainly rich in Mo, Nb, and Ti, while the interdendritic regions were enriched with Cr and Hf. Moreover, the 1–2 μm thick

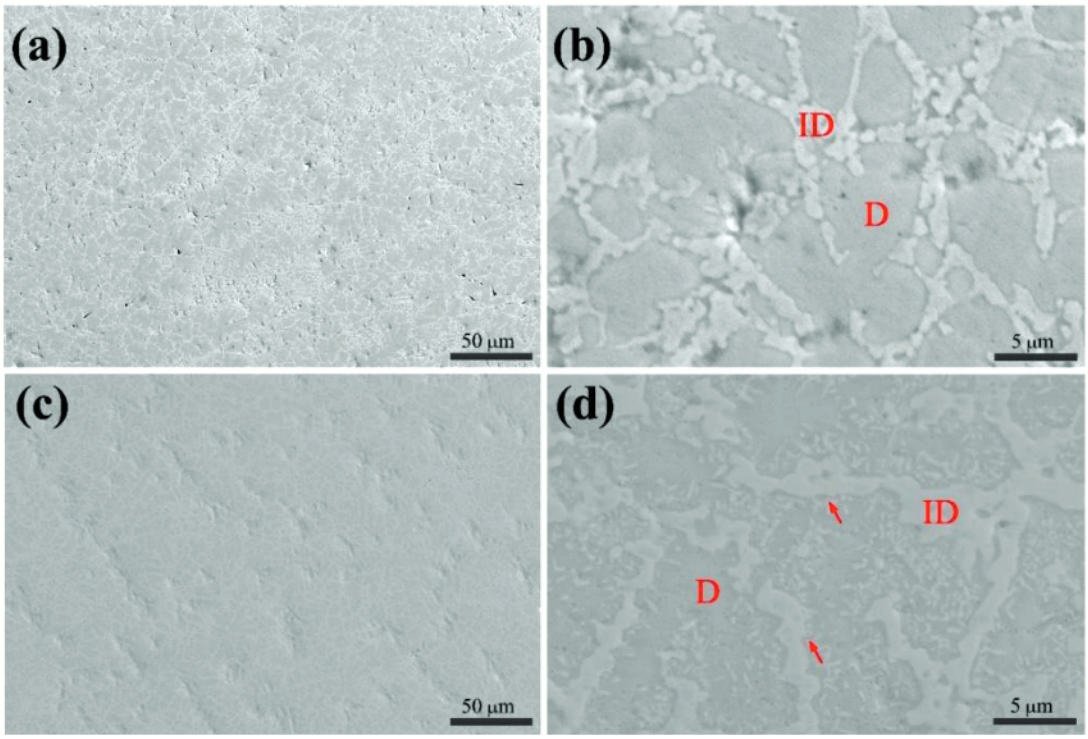

Figure 2: SEM images of: (a, b) as-cast and (c, d) annealed HfMoNbTiCr HEAs

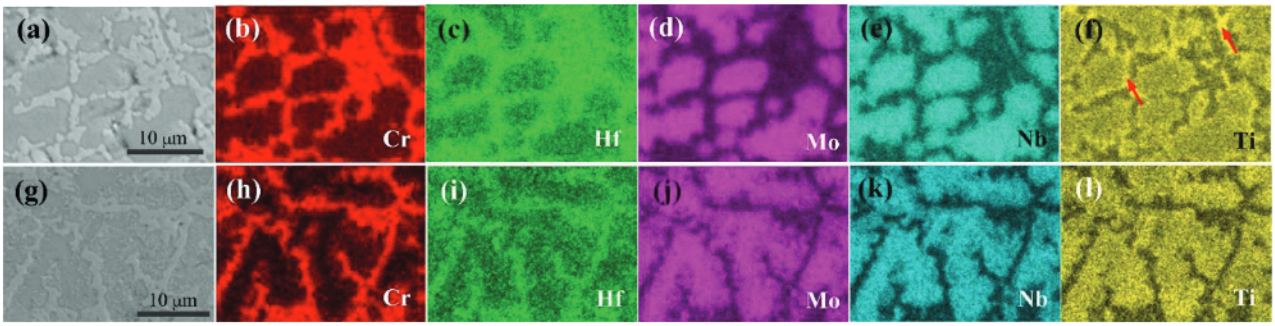

Figure 3: EDS maps of: (a–f) as-cast and (g–l) annealed HfMoNbTiCr alloy

Table 1: Quantitative chemical analysis of HfMoNbTiCr samples in the as-cast and annealed states (*a*/%)

	Region	Phase	Cr	Hf	Mo	Nb	Ti
HfMoNbTiCr -AC	D	BCC, BCC'	11.5±0.8	16.3±0.7	23.7±1.2	29.0±1.0	19.6±0.7
	D	Ti-rich layer: BCC	14.3±0.2	20.6±0.9	16.6±1.0	23.2±0.6	25.3±0.1
	ID	Laves, Laves'	37.2±1.3	26.3±0.2	10.0±0.9	11.3±0.7	15.2±0.8
HfMoNbTiCr -A	D	BCC, BCC'	7.7±1.2	15.6±0.4	23.6±2.4	29.3±0.5	23.7±2.7
	ID	Laves, Laves', BCC", HCP	36.7±3.1	27.5±0.4	14.4±1.6	9.9±1.3	11.5±0.7

Ti-rich transition layers completely disappeared after the annealing treatment.

The chemical composition derived from the EDS analysis of each region in the as-cast and annealed alloys is summarized in **Table 1**. The results strongly support the elemental-distribution determined with the mapping. Thus, combined with the phase-component analysis, the dendritic regions rich in Nb and Mo appeared to correspond to the MoNb-rich BCC phase in the as-cast HfMoNbTiCr. The interdendritic regions enriched with Cr and Hf were considered to include $(Cr, Mo)_2Hf$ Laves phases. The Ti-rich transition layers at the surface of dendrites were enriched with Ti and Nb, indicating that they were composed of a NbTi-rich BCC phase. The NbTi-rich BCC phase exhibits the same lattice structure as the MoNb-rich BCC phase, which might be the reason for the poor contrast between them in the bright-field SEM image. Likewise, for the annealed alloy, the dendritic regions rich in Nb, Mo and Ti corresponded to the Nb-rich BCC and MoTi-rich BCC' phases, while the interdendritic regions rich in Cr and Hf were considered to include $(Cr, Mo)_2Hf$ Laves phases, a Cr-rich BCC'' phase, and a Hf-rich HCP phase.

Considering the elemental distribution and melting temperature, the solidification process suggests that the high-melting-point MoNb-rich BCC phase rejected Ti, Cr and Hf into the grain boundaries (melting temperatures: Mo 2896 K, Nb 2750 K, Hf 2506 K, Cr 2180 K and Ti 1941 K). The Cr- and Hf-rich grain boundaries subsequently underwent a phase transformation that formed Cr-rich Laves phases. The Ti-rich BCC phase with the lowest melting temperature was finally extruded as a thin layer between dendrites and interdendrites. Annealing caused Ti to decompose from the original NbTi-rich BCC phase and form more of the MoTi-rich BCC' phase. This system has a low Gibbs energy due to the negative enthalpy of Mo-Ti (-4 kJ/mol) compared with the positive enthalpy of Nb-Ti (2 kJ/mol).

3.3 Compressive properties

The engineering stress-strain curves of the as-cast and annealed HfMoNbTiCr, together with those of the HfZrNbTiCr and HfMoNbTiZr alloys from the references[6,20], are shown in **Figure 4**. As expected, HfMoNbTiCr exhibited the highest strength in both the as-cast and annealed states, increasing from 1719 MPa of HfMoNbTiZr and 1375 MPa of HfNbTiCrZr to 1851 MPa of the as-cast HfMoNbTiCr, and from 1575 MPa of annealed HfMoNbTiZr to 1647 MPa of the annealed alloy. The plastic strains of all the HfNbTi-based refractory HEAs reported here, including HfMoNbTiCr (3 % in the as-cast state), HfMoNbTiZr and HfNbTiCrZr, are no more than 5 %.

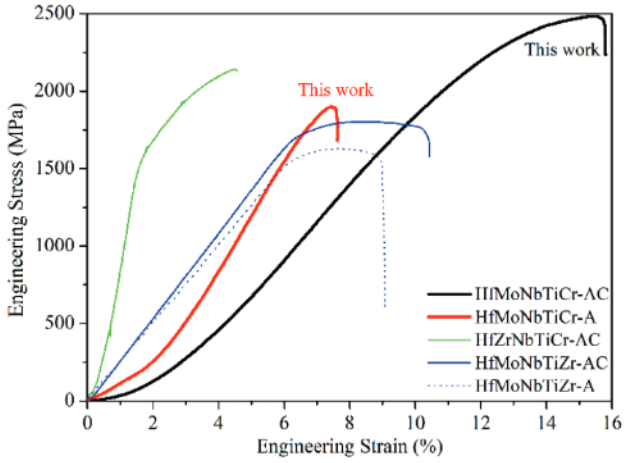

Figure 4: Engineering stress-strain curves of the as-cast and annealed HfMoNbTiCr, together with those of the reported HfZrNbTiCr and HfMoNbTiZr alloys[6,20]

As mentioned above, the phase components of HfMoNbTiZr were identical to those of HfNbTaTiZr, but the yield strength dramatically increased from 929 MPa (HfNbTaTiZr) to 1719 MPa due to elemental substitution. Such an enhancement is commonly attributed to the strong stress field caused by the different Young's modulus of Mo and other principal elements. The Young's modulus of Mo is nearly three times higher than that of Nb and Ti. In this work, the studied alloy HfMoNbTiCr was designed by replacing Zr with Cr or Mo in HfMoNbTiZr and HfZrNbTiCr. According to the phase analysis above, the incorporation of Mo in the BCC phase was not affected by the absence or incorporation of Cr, confirming that the stress field played a vital role in enhancing the yield strength. Additionally, Cr mainly segregated into the interdendritic regions, which surrounded the dendritic regions to form a netlike framework.

Alternatively, the framework might restrict the deformation, which can help further improve the yield strength. Thus, after replacing Zr with Cr and Mo, the yield strength and ultimate compressive strength of HfMoNbTiCr further increased to 1854 MPa and 2489 MPa from 1719 MPa and 1803 MPa of HfMoNbTiZr without decreasing the ductility. Besides, unlike the interdendritic regions without Mo, Nb and Ti in the annealed alloy, the corresponding regions in the as-cast alloy were enriched with Cr and the other three elements. This implies that the phase components in the dendritic regions are simpler, which might indicate that the HCP phases precipitated during annealing increased the stiffness of the framework. Moreover, Ti-rich layers surrounded the dendrites in the as-cast alloys, which might have constrained crack expansion. These phase components and microstructures increased the yield strength of the as-cast alloys compared with that of the alloy treated with annealing and subsequent strengthening.

4 CONCLUSIONS

The phase components of the as-cast HfMoNbTiCr alloy changed from a single BCC phase in the HfNbTaTiZr and HfMoNbTiZr alloys to multiple phases (mainly two BCC and two Laves phases) through elemental substitution. The yield strength of the as-cast alloy increased from 929 MPa of HfNbTaTiZr and 1719 MPa of HfNbMoTiZr to 1851 MPa while retaining a ductility of around 3.0 %. The enhanced strength may have resulted from the stress field induced by the incorporation of Mo, which formed a BCC phase, as well as the deformation constraints from the netlike framework composed of an intrinsically strong Cr-containing Laves phase. Moreover, the complexity of the framework may have decreased its stiffness, which may have helped retain some of its ductility.

Acknowledgment

Financial support from the Natural Science Foundation of the Jiangsu Province (Grants No. BK20181047) and the Natural Science Research of Jiangsu Higher Education Institutions (Grants No. 18KJB430012) are gratefully acknowledge.

5 REFERENCES

[1] D. B. Miracle, O. N. Senkov, A critical review of high entropy alloys and related concepts, Acta Materialia, 122 (**2017**) 448–511, doi:10.1016/j.actamat.2016.08.081

[2] M. H. Tsai, J. W. Yeh, High-entropy alloys: a critical review, Materials Research Letters, 2 (**2014**) 3, 107–123, doi:10.1080/21663831.2014.912690

[3] Y. Zhang, T. T. Zuo, Z. Tang, M. C. Gao, K. A. Dahmen, P. K. Liaw, Z. P. Lu, Microstructures and properties of high-entropy alloys, Progress in Materials Science, 61 (**2014**) 1–93, doi:10.1016/j.pmatsci.2013.10.001

[4] J. Yi, S. Tang, M. Xu, L. Yang, L. Wang, L. Zeng, A novel $Al_{0.5}CrCuNiV$ 3d transition metal high-entropy alloy: Phase analysis, microstructure and compressive properties, Journal of Alloys and Compounds, 846 (**2020**) 156466, doi:10.1016/j.jallcom.2020.156466

[5] O. N. Senkov, S. V. Senkova, D. B. Miracle, C. Woodward, Mechanical properties of low-density, refractory multi-principal element alloys of the Cr–Nb–Ti–V–Zr system, Materials Science and Engineering: A, 565 (**2013**) 51–62, doi:10.1016/j.msea.2012.12.018

[6] É. Fazakas, V. Zadorozhnyy, L. K. Varga, A. Inoue, D. V. Louzguine-Luzgin, F. Tian, L. Vitos, Experimental and theoretical study of $Ti_{20}Zr_{20}Hf_{20}Nb_{20}X_{20}$ (X=V or Cr) refractory high-entropy alloys, International Journal of Refractory Metals and Hard Materials, 47 (**2014**) 131–138, doi:10.1016/j.ijrmhm.2014.07.009

[7] O. N. Senkov, C. Woodward, D. B. Miracle, Microstructure and Properties of Aluminum-Containing Refractory High-Entropy Alloys, JOM, 66 (**2014**) 10, 2030–2042, doi:10.1007/s11837-014-1066-0

[8] O. N. Senkov, S. V. Senkova, C. Woodward, Effect of aluminum on the microstructure and properties of two refractory high-entropy alloys, Acta Materialia, 68 (**2014**) 214–228, doi:10.1016/j.actamat.2014.01.029

[9] B. Gorr, M. Azim, H. J. Christ, T. Mueller, D. Schliephake, M. Heilmaier, Phase equilibria, microstructure, and high temperature oxidation resistance of novel refractory high-entropy alloys, Journal of Alloys and Compounds, 624 (**2015**) 270–278, doi:10.1016/j.jallcom.2014.11.012

[10] J. W. Yeh, S. K. Chen, S. J. Lin, J. Y. Gan, T. S. Chin, T. T. Shun, S. Y. Chang, Nanostructured high-entropy alloys with multiple principal elements: novel alloy design concepts and outcomes, Advanced Engineering Materials, 6 (**2004**) 299–303, doi:10.1002/adem.200300567

[11] B. Cantor, I. T. H. Chang, P. Knight, A. J. B. Vincent, Microstructural development in equiatomic multicomponent alloys, Materials Science and Engineering: A, 375–377 (**2004**) 213–218, doi:10.1016/j.msea.2003.10.257

[12] O. N. Senkov, G. B. Wilks, D. B. Miracle, C. P. Chuang, P. K. Liaw, Refractory high-entropy alloys, Intermetallics, 18 (**2010**) 9, 1758–1765, doi:10.1016/j.intermet.2010.05.014

[13] O. N. Senkov, G. B. Wilks, J. M. Scott, D. B. Miracle, Mechanical properties of $Nb_{25}Mo_{25}Ta_{25}W_{25}$ and $V_{20}Nb_{20}Mo_{20}Ta_{20}W_{20}$ refractory high entropy alloys, Intermetallics, 19 (**2011**) 5, 698–706, doi:10.1016/j.intermet.2011.01.004

[14] O. N. Senkov, J. M. Scott, S. V. Senkova, D. B. Miracle, C. F. Woodward, Microstructure and room temperature properties of a high-en-

tropy TaNbHfZrTi alloy, Journal of Alloys and Compounds, 509 (**2011**) 20, 6043–6048, doi:10.1016/j.jallcom.2011.02.171

[15] X. Jin, Y. Liang, J. Bi, B. Li, Non-monotonic variation of structural and tensile properties with Cr content in AlCoCrxFeNi2 high entropy alloys, Journal of Alloys and Compounds, 798 (**2019**) 243–248, doi:10.1016/j.jallcom.2019.05.211

[16] M. G. Poletti, G. Fiore, B. A. Szost, L. Battezzati, Search for high entropy alloys in the X-NbTaTiZr systems (X=Al, Cr, V, Sn), Journal of Alloys and Compounds, 620 (**2015**) 283–288, doi:10.1016/j.jallcom.2014.09.145

[17] Y. Chen, S. Zhu, X. Wang, B. Yang, Z. Ren, G. Han, S. Wen, The strength-ductility balance of $Al_{0\text{-}4}CoCu_{0.6}NiTi_x$ (x=1.0) and $Al_{0\text{-}4}CoCu_{0\text{-}6}NiSi_{0.2}Ti_x$ (x=0.5) high entropy alloys by regulating the proportion of Ti and improving the cooling rate, Vacuum, 155 (**2018**) 270–279, doi:10.1016/j.vacuum.2018.06.020

[18] N. D. Stepanov, N. Y. Yurchenko, D. V. Skibin, M. A. Tikhonovsky, G. A. Salishchev, Structure and mechanical properties of the AlCrxNbTiV (x = 0, 0.5, 1, 1.5) high entropy alloys, Journal of Alloys and Compounds, 652 (**2015**) 266–280, doi:10.1016/j.jallcom.2015.08.224

[19] C. M. Lin, C. C. Juan, C. H. Chang, C. W. Tsai, J. W. Yeh, Effect of Al addition on mechanical properties and microstructure of refractory $Al_xHfNbTaTiZr$ alloys, Journal of Alloys and Compounds, 624 (**2015**) 100–107, doi:10.1016/j.jallcom.2014.11.064

[20] N. N. Guo, L. Wang, L. S. Luo, X. Z. Li, Y. Q. Su, J. J. Guo, H. Z. Fu, Microstructure and mechanical properties of refractory MoNbHfZrTi high-entropy alloy, Materials & Design, 81 (**2015**) 87–94, doi:10.1016/j.matdes.2015.05.019

[21] A. Inoue, Stabilization of metallic supercooled liquid and bulk amorphous alloys, Acta Materialia, 48 (**2000**) 279–306, doi:10.1016/S1359-6454(99)00300-6

[22] O. N. Senkov, C. F. Woodward, Microstructure and properties of a refractory $NbCrMo_{0.5}Ta_{0.5}TiZr$ alloy, Materials Science and Engineering: A, 529 (**2011**) 311–320, doi:10.1016/j.msea.2011.09.033